



MRI Supervised and Unsupervised Classification of Parkinson's Disease and Multiple System Atrophy

Patrice Péran, PhD ^{1*}, Gaetano Barbagallo, MD,² Federico Nemmi, PhD,¹ Maria Sierra, MD,³ Monique Galitzky, MD,⁴ Anne Pavy-Le Traon, MD, PhD,^{5,6} Pierre Payoux, MD, PhD,¹ Wassilios G. Meissner, MD, PhD ^{7,8,9} and Olivier Rascol, MD, PhD^{1,10}

¹ToNIC, Toulouse NeuroImaging Center, Université de Toulouse, Inserm, UPS, France

²Institute of Neurology, University Magna Græcia, Catanzaro, Italy

³Neurology Service, University Hospital Marqués de Valdecilla and Centro de Investigación Biomédica en Red de Enfermedades Neurodegenerativas (CIBERNED), Santander, Spain

⁴Centre d'Investigation Clinique (CIC), CHU de Toulouse, Toulouse, France

⁵UMR Institut National de la Santé et de la Recherche Médicale 1048, Institut des Maladies Métaboliques et Cardiovasculaires, Toulouse, France

⁶Department of Neurology and Institute for Neurosciences, University Hospital of Toulouse, Toulouse, France

⁷Service de Neurologie, CHU Bordeaux, Bordeaux, France

⁸Univ. de Bordeaux, Institut des Maladies Neurodégénératives, UMR 5293, Bordeaux, France

⁹CNRS, Institut des Maladies Neurodégénératives, UMR 5293, Bordeaux, France

¹⁰Université de Toulouse 3, CHU de Toulouse, INSERM, Centre de Référence AMS, Service de Neurologie et de Pharmacologie Clinique, Centre d'Investigation Clinique CIC1436, Réseau NS-Park/FCRIN et Centre of excellence for neurodegenerative disorders (COEN) de Toulouse, Toulouse, France

ABSTRACT: Background: Multimodal MRI approach is based on a combination of MRI parameters sensitive to different tissue characteristics (eg, volume atrophy, iron deposition, and microstructural damage). The main objective of the present study was to use a multimodal MRI approach to identify brain differences that could discriminate between matched groups of patients with multiple system atrophy, Parkinson's disease, and healthy controls. We assessed the 2 different MSA variants, namely, MSA-P, with predominant parkinsonism, and MSA-C, with more prominent cerebellar symptoms.

Methods: Twenty-six PD patients, 29 MSA patients (16 MSA-P, 13 MSA-C), and 26 controls underwent 3-T MRI comprising T2*-weighted, T1-weighted, and diffusion tensor imaging scans. Using whole-brain voxel-based MRI, we combined gray-matter density, T2* relaxation rates, and diffusion tensor imaging scalars to compare and discriminate PD, MSA-P, MSA-C, and healthy controls.

Results: Our main results showed that this approach reveals multiparametric modifications within the cerebellum and putamen in both MSA-C and MSA-P patients, compared with PD patients. Furthermore, our findings revealed that specific single multimodal MRI markers were sufficient to discriminate MSA-P and MSA-C patients from PD patients. Moreover, the unsupervised analysis based on multimodal MRI data could regroup individuals according to their clinical diagnosis, in most cases.

Conclusions: This study demonstrates that multimodal MRI is able to discriminate patients with PD from those with MSA with high accuracy. The combination of different MR biomarkers could be a great tool in early stage of disease to help diagnosis. © 2018 International Parkinson and Movement Disorder Society

Key Words: Parkinson's disease; multiple system atrophy; MRI; iron; diffusion tensor imaging

Multiple system atrophy (MSA) and Parkinson's disease (PD) are 2 neurodegenerative disorders characterized by the accumulation of α -synuclein aggregates,

primarily in neurons in PD and in oligodendrocytes in MSA.¹ The clinical diagnosis of MSA can be challenging, as no specific symptom or biomarker allows a

*Correspondence to: Patrice Péran, UMR 1214 - INSERM/UPS - ToNIC, Toulouse NeuroImaging Center, CHU PURPAN - Pavillon Baudo - Place du Dr Baylac, 31024 Toulouse - Cedex 3, France; patrice.peran@inserm.fr

Relevant conflicts of interest/financial disclosures: Nothing to report.
Funding agencies: The study was sponsored by Inserm and funded by a "Recherche clinique translationnelle" grant from INSERM-DGOS (2013-2014).

Received: 16 November 2017; **Revised:** 15 December 2017;
Accepted: 22 December 2017

Published online 00 Month 2018 in Wiley Online Library (wileyonlinelibrary.com). DOI: 10.1002/mds.27307

“definite” diagnosis *in vivo*. Currently, the “definite” diagnosis of MSA requires postmortem confirmation by a neuropathological examination. It is often challenging in clinical practice to differentiate MSA, especially its parkinsonian variant (MSA-P), from PD, as both entities can share similar phenotypes, especially in early stages. Importantly, these disorders have dramatically different prognoses in terms of disability, therapeutic response, and survival. International consensus criteria have been developed, allowing the diagnosis of “probable” or “possible” MSA, based on clinical or a combination of clinical and imaging features, respectively.² However, more specific and sensitive biomarkers, allowing better differentiation between MSA and PD are still needed to improve diagnostic accuracy.

Conventional MRI (ie, clinical T1- and T2-weighted imaging) has been used extensively to identify diagnostic markers of PD and MSA. Brain MRI is substantially normal in patients with PD,³ even if advanced MRI methods can discriminate PD patients from healthy controls.⁴⁻⁶ In patients with MSA, characteristic MR signs include putaminal atrophy and T2 hypointensity, with a slitlike marginal hyperintensity of the putamen, atrophy of the middle cerebellar peduncles, pons, and cerebellum, and a pontine cruciform hyperintensity (hot cross bun sign) on T2-weighted and proton density-weighted images.³ These markers have relatively good specificity but only low sensitivity.⁷ Previous neuroimaging studies have investigated automatic classification tools based on MRI volumetric parameters to discriminate patients with different parkinsonian syndromes, including MSA and PD.^{8,9} Such studies emphasize the importance of studying cerebellum, brain stem, and putamen volumetric parameters extracted from T1-weighted images to discriminate MSA and PD patients. However, the only published study that specifically examined a subgroup of patients suffering from the MSA-P variant, the most challenging condition for diagnostic discrimination from PD, only reported a rather moderate separation between both conditions (discriminant power, 71.9%) with a low separability of PD from controls.⁹ A recent work using a new parameter from diffusion imaging showed high discriminant power between PD and MSA.¹⁰ However, the values were calculated from manually drawn regions of interest that cannot be used in an automatic pipeline. Other quantitative multiparametric MRI imaging techniques, exploring macrostructural and microstructural modifications in the basal ganglia and mesencephalon and using different types of modalities for acquisition and image processing, also provided promising findings.⁵ The multimodal MRI (mMRI) approach is designed to overcome the limitations of previous single MR-parameter studies. The mMRI approach concept is based on the combination of MRI parameters from different MRI sequences that are sensitive to different tissue characteristics (eg, volume atrophy, iron deposition, and microstructural damage). Using a combination

of 3 different markers (relaxometry in the substantia nigra, fractional anisotropy in the substantia nigra, and mean diffusivity in the putamen or caudate nucleus), we were able to distinguish PD patients from healthy controls.⁵ We hypothesize that a similar approach is a promising tool to separate MSA from PD patients.

The main objective of the present study was to use an mMRI approach to identify brain differences that could discriminate between matched groups of patients with MSA, PD, and healthy controls. We carefully assessed the 2 different MSA variants, namely, MSA-P, with predominant parkinsonism, and MSA-C, with more prominent cerebellar symptoms. Using whole-brain voxel-based MRI, we combined gray-matter density, T2* relaxation rates, and diffusion tensor imaging (DTI) scalars to compare and discriminate PD, MSA-P, MSA-C, and healthy controls. We also assessed the capacity of an unsupervised machine-learning method by using multiparametric imaging data to classify our subjects without using any clinical label.

Methods

Subjects

Twenty-nine MSA and 26 PD patients matched for age and sex were prospectively recruited at the outpatient clinic of the Toulouse PD Expert Center and the Toulouse site of the French Reference Center for MSA (details in Supplemental data). Inclusion criteria were: (1) diagnosis of PD or MSA according to established international diagnostic criteria^{2,11}; (2) Hoehn and Yahr score¹² < 4 on treatment; (3) negative history of neurological or psychiatric diseases other than PD or MSA; (4) lack of significant cognitive decline (Mini Mental State Examination score > 24); (5) no treatment with deep brain stimulation; and (6) no evidence of movement artifacts, vascular brain lesions, brain tumor, and/or marked cortical and/or subcortical atrophy on MRI scan (2 expert radiologists examined all MRIs to exclude potential brain abnormalities as apparent on conventional FLAIR, T2-weighted, and T1-weighted images). A healthy control group of 26 right-handed subjects closely matched to patients for age, sex, and education was also included.

Two subgroups were identified within the MSA total group (MSA-tot), according to international consensus diagnostic criteria²: an MSA-P subgroup (n = 16) and an MSA-C subgroup (n = 13). Among the MSA-matched PD total group (PD-tot), 2 subgroups were generated: a PD-p subgroup (n = 16) and a PD-c subgroup (n = 13) to better match MSA-P and MSA-C, respectively, for sex, age, and disease duration. All patients were assessed by MSA and PD specialists, and the clinical diagnosis was confirmed 2 years after MRI data acquisition (further details in Supplemental data).

The L-dopa-equivalent daily dose was calculated for each patient.¹³ Motor disability was assessed using motor examination scores of the Unified Parkinson's Disease Rating Scale-III¹⁴ and of the Unified MSA Rating Scale-II.² All patients receiving antiparkinsonian treatments were tested on medication.

The study was conducted according to the Declaration of Helsinki and approved by the Toulouse Ethics Committee. Written informed consent was obtained from all participants.

Acquisition

We used an mMRI protocol similar to our previous study (Péran et al, 2010), that is, T1, T2 relaxometry, DTI (details in Supplemental data).

Postprocessing

Image processing was performed using FSL v5 (www.fmrib.ox.ac.uk/fsl/) and an in-house-developed software in Matlab, with procedures similar to those described previously.^{5,15,16} (details in Supplemental data). As a result of this processing, the grey density (GD), mean diffusivity (MD), fractional anisotropy (FA), and R2* maps were generated in the Montreal Neurological Institute (MNI) space.

Statistical Analysis

Voxel-Based Analysis

The GD, R2*, MD, and FA maps were compared using nonparametric 2-sample unpaired *t* tests (FSL-randomize¹⁷: PD versus MSA-tot, HC versus PD-tot, HC versus MSA-tot, PD-p versus MSA-P, PD-c versus MSA-C, MSA-P versus MSA-C. The statistical significance threshold was set to $P < 0.01$ corrected for family-wise error using the threshold-free cluster-enhancement approach,¹⁸ with a minimum cluster size equal to 20 voxels. For each significant cluster associated with a specific MR parameter (GD, R2*, MD, or FA), the mean values of that parameter were extracted for all participants.

Discriminant Analysis and Receiver Operating Characteristic Curves

Because one of the main goals of the study was to discriminate PD from MSA patients, we used logistic regressions and receiver operating characteristic (ROC) curves to discriminate between the clinical groups. Both logistic regressions and ROC curves were computed using the mean of each MR parameter/cluster pair from the previous voxel-based analysis in each individual. All combinations among these pairs were tested to determine the combinations with the best discriminating power. A repeated 10-fold cross-validation was performed to calculate the area under the ROC curve (AUC) for each combination. Combinations with AUC > 95% are reported.

Unsupervised Classification

Another goal of the study was to determine if neuroimaging data from mMRI could be used to classify patients independently from clinical data. Therefore, we computed the self-organizing map (SOM) method or Kohonen map, a type of clustering method using unsupervised learning, with the same set of features used for supervised analysis, that is, the averages of each MR parameter/subregion pair individualized from the previous voxel-based analysis (PD-tot versus HC, PD-tot versus MSA-tot, MSA-tot versus HC, MSA-P versus MSA-C); for details, see Supplemental data.

Results

Clinical Comparisons Between Groups

Table 1 summarizes the demographic and clinical characteristics of HC, PD, and MSA subjects. Nine of 13 MSA-C patients did not receive any antiparkinsonian therapy.

mMRI Differences Between MSA and PD Patients

MSA-tot Versus PD-tot

Patients with MSA showed lower GD value clusters within the cerebellum, the putamen, and the supplementary motor area (SMA) bilaterally and in the left middle and anterior cingulate cortices. In addition, MSA patients showed higher R2* clusters in the putamen bilaterally and higher MD values and lower FA values in large clusters within the cerebellum, the brain stem, the superior corona radiata, the body of the corpus callosum, and the external and internal capsules (see Fig. 1).

MSA-P Versus PD-p (Fig. 2)

MSA-P patients displayed (1) lower GD in the putamen and in the SMA bilaterally, (2) higher R2* values in the right putamen, and (3) higher MD values in the cerebellum (mainly Crus I-II, lobe VI bilaterally), the putamen, and the superior corona radiata bilaterally. Further, MSA patients showed lower FA values in the right putamen, the left middle cerebellar peduncle, the superior corona radiata bilaterally, and the body of the corpus callosum.

MSA-C Versus PD-c (Fig. 2)

Patients with MSA-C showed lower GD, higher MD, and lower FA values in the cerebellum, as well as clusters of lower GD values in the posterior cingulate cortex and higher MD values in the left cerebral peduncle and pallidum.

TABLE 1. Demographic and clinical characteristics of healthy controls and patients with Parkinson’s disease and Multiple System Atrophy.

group	n	sex (M/F)	age, y (mean ± SD)	disease duration, y (mean ± SD)	LEDD (mean ± SD)	UPDRS-III (mean ± SD)	UMSARS-II (mean ± SD)
PD	26	12/14	63.8 ± 6.3	7.4 ± 4.5	689.0 ± 367.2	19.1 ± 10.0	-
MSA-tot	29	13/16	64.0 ± 7.5	5.7 ± 2.3	470.4 ± 500.5	-	29.8 ± 8.0
HC	26	11/15	66 ± 4,9	NA	NA	NA	NA
<i>p value</i>		<i>ns</i>	<i>ns</i>	<i>ns</i>	0.03*	NA	NA
PD-matched	16	7/9	65.1 ± 6.8	8.3 ± 4.5	712.5 ± 327.8	22.0 ± 11.2	-
MSA-P	16	7/9	66.1 ± 7.8	5.4 ± 2.2	700.1 ± 386.4	-	31.1 ± 8.7
<i>p value</i>		<i>ns</i>	<i>ns</i>	<i>ns</i>	<i>ns</i>	NA	NA
PD-matched	13	6/7	61.6 ± 4.2	7.5 ± 4.6	754.4 ± 405.0	16.8 ± 10.4	-
MSA-C	13	6/7	61.5 ± 6.5	6.1 ± 2.5	187.8 ± 490.8	-	28.2 ± 7.0
<i>p value</i>		<i>ns</i>	<i>ns</i>	<i>ns</i>	0.0004**	NA	NA
MSA-P	16	7/9	66.1 ± 7.8	5.4 ± 2.2	700.1 ± 386.4	-	31.1 ± 8.7
MSA-C	13	6/7	61.5 ± 6.5	6.1 ± 2.5	187.8 ± 490.8	-	28.2 ± 7.0
<i>p value</i>		<i>ns</i>	<i>ns</i>	<i>ns</i>	0.0003**	-	<i>ns</i>

M = male; F = female. MMSE = Mini Mental State Examination. LEDD = levodopa equivalent daily dose. UPDRS-III = third part of UPDRS (Unified Parkinson’s Disease Rating Scale). UMSARS-II = second part of UMSARS (Unified Multiple System Atrophy Rating Scale). PD = Parkinson’s disease. MSA = Multiple System Atrophy. MSA-C = cerebellar variant of MSA. MSA-P = parkinsonian variant of MSA. PD-p = PD subgroup matched with MSA-P subgroup for sex, age, and disease duration. PD-c = PD subgroup matched with MSA-C subgroup for sex, age, and disease duration. *ns* = not significant. *NA* = not applicable. Significant *p-values* are indicated in bold (signed *Mann-Whitney U* test).

MSA-C Versus MSA-P (Fig. 2)

MSA-C patients showed lower GD, higher MD, and lower FA values in the cerebellum, higher R2* clusters in the right cerebellum, internal capsule and thalamus, and lower MD clusters in the right putamen.

The Supplemental Table reports cluster localization, size, MNI coordinates, and mean values in the PD and MSA samples for each cluster.

The results of the comparisons between patients and HCs are reported in the Supplemental data.

Discriminant Analysis

Global Group Analyses: MSA-tot Versus PD-tot

Logistic regression analysis showed that combining 2 different markers was enough to obtain >95%

discrimination between PD and MSA patients. Specifically, this accuracy was reached including the following clusters: (FA/cerebellum, brain stem, and WM bilateral superior corona radiata) + (MD/right superior frontal gyrus). Logistic regression was also computed for combinations of 3 markers. Including a third marker did not significantly increase the discriminating power (maximum AUC, 96%).

Subgroup Analyses: MSA-P Versus PD-p

Logistic regression analysis showed that including a single marker at a time was enough to obtain >95% discrimination between MSA-P and PD-p matched patients. Five markers reached this threshold: GM/bilateral SMA, MD/SMA, and left corona radiata, MD/cerebellum, FA/left

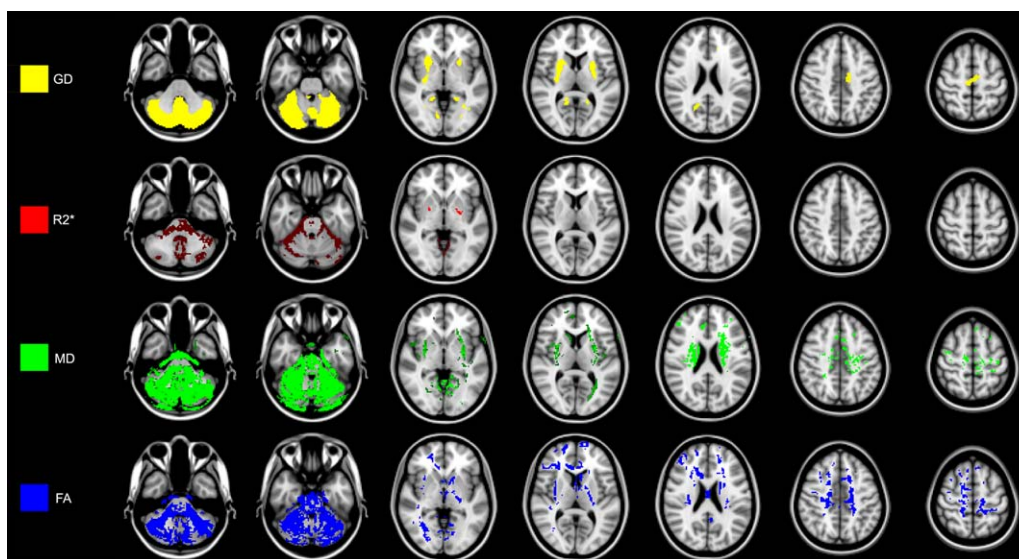


FIG. 1. Differences between patients with PD and patients with MSA from voxel-based analysis of GD, R2*, MD and FA maps. [Color figure can be viewed at wileyonlinelibrary.com]

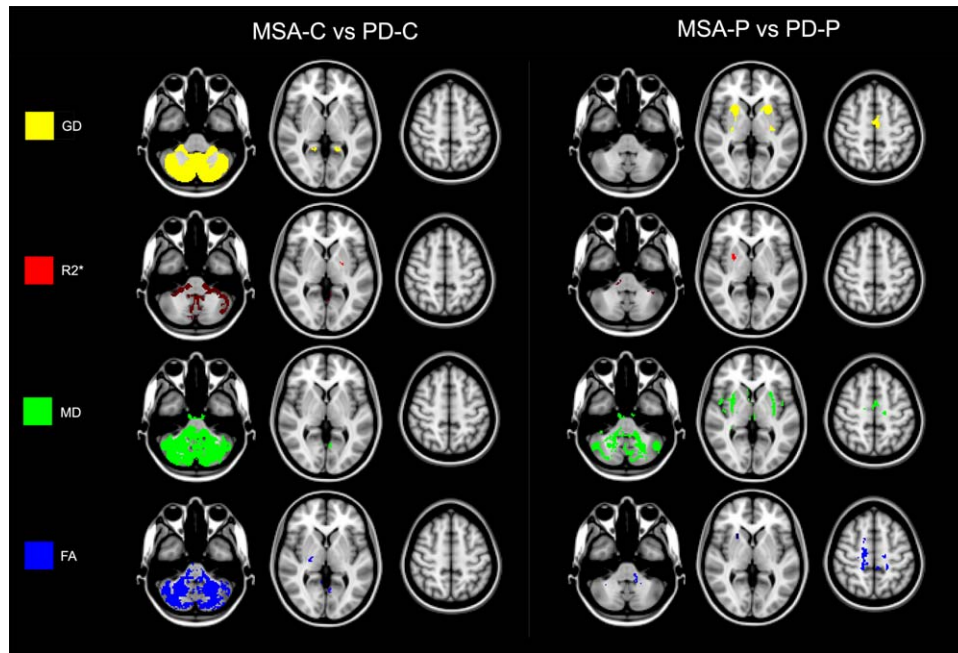


FIG. 2. Differences between patients with PD and patients with MSA-P and MSA-C from voxel-based analysis of GD, R2*, MD and FA maps. [Color figure can be viewed at wileyonlinelibrary.com]

corona radiata, FA/right corona radiata (Fig. 3A). Logistic regression was also computed for combinations of 2 markers (see Supplementary data).

Subgroup Analyses: MSA-C Versus PD-c

Logistic regression analysis showed that including a single marker at a time was enough to obtain >95% discrimination between MSA-C and PD-c patients. Four markers reached this threshold: GM/cerebellum, R2*/cerebellum, R2*/left cerebral peduncle, MD/cerebellum (Fig. 3B).

Unsupervised Classification

Figure 4 shows the distribution of patients in SOM-2 × 2. For each map, each cluster is represented by $S_{[i,j]}$, where i and j are the row and column numbers of the cluster, respectively. Each item represents a patient. For a

better interpretation, the clinical diagnosis was tagged a posteriori. In all clusters $S_{2,2}$, a high population of patients with the same clinical diagnosis, is observed. The cluster $S_{1,2}$ included all HC participants. Only 2 PD patients were part of this cluster. The cluster $S_{2,1}$ included only PD patients. The clusters $S_{1,1}$ and $S_{2,2}$ were mainly formed of MSA patients. More precisely, the cluster $S_{2,2}$ consisted essentially of MSA-C patients with the presence of 2 MSA-P patients. The cluster $S_{1,1}$, which was composed predominantly of MSA-P patients, and included 2 PD and 2 MSA-C patients.

Discussion

Our main results showed that this approach reveals multiparametric modifications within the cerebellum

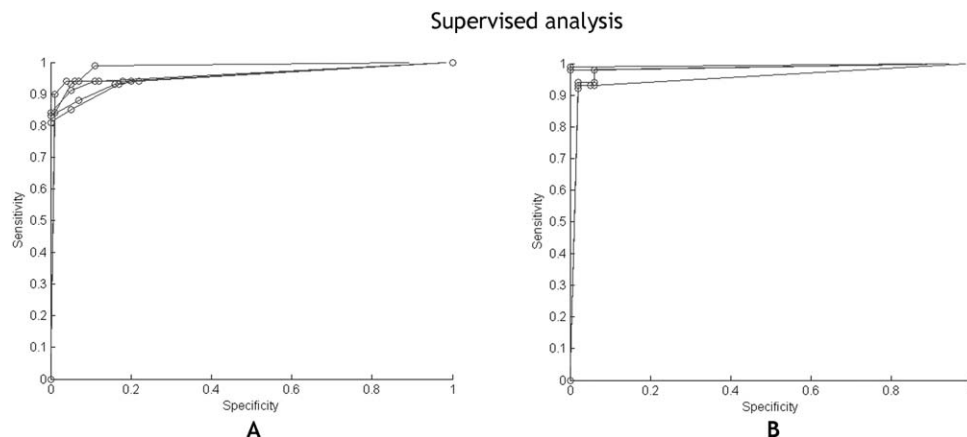


FIG. 3. (A–B) ROC curves associated with each significant combination (>95%) in discriminating (A) MSA-P from PD patients and (B) MSA-C from PD patients.

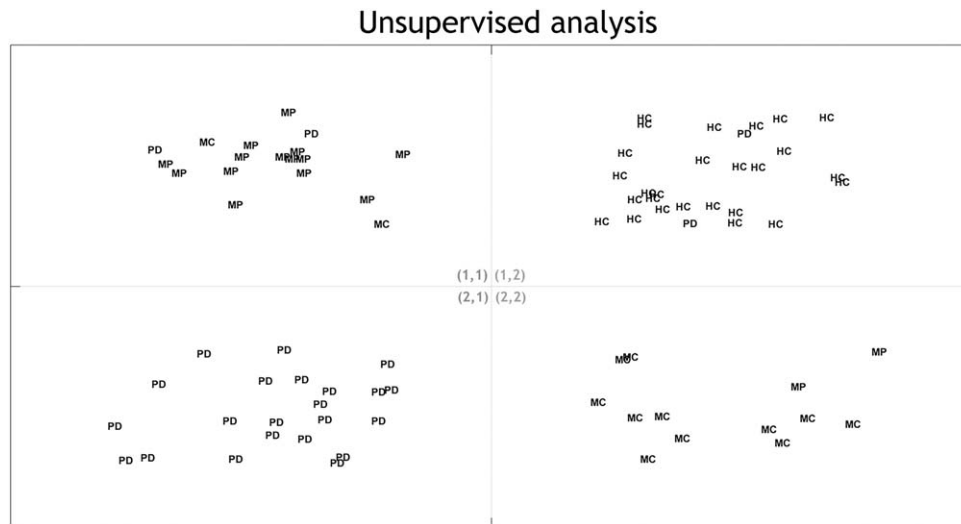


FIG. 4. Kohonen maps of patients showing sample distribution on the map and the assigned groups to samples for a SOM-2x2 network. PD: PD patients; MP: MSA-P patients; MC: MSA-C patients; HC: Controls.

and putamen in both MSA-C and MSA-P as compared with PD patients. Furthermore, our findings revealed that specific single mMRI markers were sufficient to discriminate MSA-P and MSA-C patients from PD patients. Moreover, the unsupervised analysis was based on mMRI data, which could regroup individuals according to their clinical diagnosis, in most cases. This latter finding shows that a classification based on MRI findings blind to the clinical diagnosis can provide consistent and coherent clusters of subjects.

Discriminant Markers

The results of the ROC and cross-validated discrimination analyses demonstrated that several combinations of 2 different markers were sufficient to obtain >95% discrimination between MSA and PD patients. The markers comprising the discriminating combinations were both supra- and infratentorial, including FA in the cerebellum, brain stem, and superior corona radiata and MD in the right superior frontal gyrus. Unsurprisingly, the main predictive markers involved the infratentorial structures that characterize MSA pathology, such as the cerebellum and brain stem. In addition, our results also showed a contribution of supratentorial damage (superior corona radiata and superior frontal gyrus) for the differentiation between patients with MSA. These results are in agreement with recent studies also showing that automated MRI analysis discriminates between PD and MSA patients.^{8,9} Unlike in our study, these studies only used one MRI modality (T1-weighted imaging to perform volumetry). Using a decision tree approach that considered volume loss of the more affected cerebellar gray-matter compartment and putamen as well as the absence of severe midbrain atrophy, all patients with MSA of the test set were correctly classified.⁸ The

anatomical structures involved in this automated MRI analysis were the same highlighted by our data-driven approach. However, the study of Scherfler and colleagues (2016) did not investigate the ability of MRI indexes to discriminate between the 2 MSA subgroups and PD patients. The results of the ROC and cross-validated discrimination analyses demonstrated that 1 marker was enough to reach 95% of discriminant power between MSA-P and PD patients. The discriminant markers that allowed for 95% of discriminant power were the MD in the cerebellum, FA and GD in the putamen, GD in the supplementary motor area, and FA in the superior corona radiata. Overall, these results confirmed the prevalence of supratentorial involvement in the MSA-P variant (ie, putamen, supplementary motor area, and superior corona radiata), even though MD allowed us to detect the presence of infratentorial microstructural damage (ie, cerebellum). We reached a higher discriminant power between MSA-P and PD patients than found in a previous study using only 1 modality.⁹ Unsurprisingly, any cerebellar marker alone was enough to reach AUC >95% discrimination between MSA-C and PD. Overall, these results confirm the prevalence of infratentorial involvement in the MSA-C variant (ie, cerebellum). Although this result is perfectly coherent with the clinical picture of MSA-C patients, it is difficult to exclude a partial volume effect on the nonvolumetric MRI parameters (R2*, MD, and FA) because of the severe cerebellar atrophy in MSA patients. Another advantage of our discriminant analysis is the use of subregions that were the product of the whole-brain voxel-based analysis that is more sensitive to disease-associated changes. In addition, the multiparameter aspect of our approach likely explains the higher discriminant power in our study compared with previous studies based on whole anatomical region.^{8,9} In conclusion, mMRI is able to identify specific MRI

markers to discriminate patients with Parkinson's disease from patients with MSA with high accuracy.

To complement the promising results from the supervised discrimination analysis, we conducted an unsupervised analysis to sort data into data-driven categories based on mMRI data similarities only, without considering any a priori clinical information. The results of this analysis were promising on different levels. First, patients were mainly regrouped according to the clinical diagnosis (see Fig. 4). HC subjects were sorted in a unique cluster. Noteworthy, MSA patients were segregated into 2 distinct clusters in accordance with their clinical phenotype (ie, MSA-P and MSA-C). Finally, PD patients formed an independent cluster. Another interesting result of this analysis was the agreement with the clinical diagnosis and also with dissimilarities. Indeed, we observed some individuals, mainly PD patients, outside the clouds of dots corresponding to their diagnosis-related group. This may be explained by (1) false-negatives, individuals with a clinical diagnosis of PD who were associated with the cluster mainly composed of HC participants (Fig. 4 $S_{[1,2]}$); (2) a "clinical-MRI" mismatch, individuals with a clinical diagnosis of PD who were associated with the cluster with a higher population of MSA-P patients (Fig. 4 $S_{[1,1]}$). False-negatives can occur because of a certain lack of sensitivity of the method, that is, the difficulty in distinguishing PD patients from HC participants. Indeed, the diagnosis of PD is based mainly on a set of clinical assessments, and conventional MRI only aids in excluding underlying pathologies (eg, vascular lesions). For individuals with a "clinical-MRI" mismatch, these patients seem not to not share the same MRI features that the other patients with the same clinical diagnosis do. This can be for several reasons. First, the MRI data used in unsupervised analysis may not have fully characterized each patient, causing a failure in clustering. An argument against this explanation is that MRI data used in unsupervised analysis were identical to those used for discriminant analysis, which showed high sensitivity and specificity. The second line of interpretation considers that clinical diagnostic criteria are not 100% accurate, particularly in the early stage of disease.^{19,20} Finally, PD patients in the MSA-P cluster may in fact be MSA patients with milder disease.^{21,22} The only way to confirm this hypothesis would be to follow longitudinally these patients for several years and to collect and to analyze postmortem brains. Clearly, further studies will be necessary to compare neuroimaging, clinical and postmortem brain.

Spatial Patterns of mMRI Changes

Looking at the spatial patterns, the comparison between patients and HC subjects confirmed previous

results.^{5,23} The results showed a higher $R2^*$ value in the substantia nigra for PD versus HC and MSA versus HC. Numerous anatomopathological^{24,25} and MR studies^{4,5,26} have confirmed this specific iron accumulation. Recently, quantitative susceptibility mapping (QSM) method confirmed the localization of iron accumulation in PD patients.²⁷ Moreover, a previous study showed that the assessment of iron content in the dorsolateral substantia nigra may be useful for distinguishing between HCs and patients with neurodegenerative parkinsonism, including PD and MSA.²⁸ Our results did not show differences between PD patients and HCs for DTI parameters. To investigate brain changes in both MSA and PD, we chose to investigate MRI parameters by whole-brain analysis using a strict statistical significance threshold. In contrast to previous studies using a region-of-interest approach that found a decrease in FA in the substantia nigra in PD patients compared with control subjects,^{5,6,29} our methodological choice may explain the lack of differences for DTI parameters between PD and HC. However, a recent meta-analysis questioned the validity of FA in SN as a PD biomarker.³⁰

Except for the iron content in the substantia nigra, the differences in the multiparametric spatial pattern between MSA patients and HCs was almost identical to the one between MSA and PD. The multiparametric voxel-based analysis showed significant differences between both disorders. Indeed, the difference between MSA and PD patients reached a high significance level for each parameter, highlighting major differences between the disorders. Irrespective of the analyzed MR parameters, the differences between MSA and PD patients were always in the direction of more damaged brain in MSA patients. Specifically, brain regions demonstrating differences in gray-matter density corresponded to atrophy in MSA patients. Similarly, all brain regions with a difference in MD corresponded to a mean diffusivity increase in MSA patients. The spatial localization of MR changes was in keeping with previous single MR parameter studies: VBM-studies,^{31,32} MR relaxometry,^{33,34} and DTI studies^{35,36} in patients with PD and MSA.

Furthermore, comparing MSA-and MSA-C with 2 carefully matched subgroups of PD patients, we were able to show a distinct topographical distribution of macro- and microstructural changes of the 2 MSA phenotypes. Accordingly, MSA-P patients showed higher involvement of supratentorial structures than PD patients, although not exclusively. Patients with MSA-P showed putaminal atrophy (GD), macrostructural damage in the supplementary motor area (GD), and microstructural damage in the corona radiata and corpus callosum (FA), together with

exclusive microstructural damage at the infratentorial level (MD), in particular in the cerebellum and middle cerebellar peduncles, in keeping with previous studies.^{35,37-39} When comparing PD with MSA-C, unsurprisingly, we found cerebellar damage in MSA-C at the macro- and microstructural levels.⁴⁰ In this view and compared with PD, MSA-C patients showed a decrease in GM and FA values, an increase in MD values in the cerebellum, a decrease in GM values in the posterior cingulate cortex and an increase in R2* values in the pallidum and left cerebral peduncle. As previously discussed, the results from other parameters located in the cerebellum could be related to partial volume effect. This spatial pattern of mMRI changes was very similar to previous MRI results involving a single MR parameter.⁴¹ Finally, we directly compared the 2 MSA variants. Unsurprisingly, we mainly found a loss of GD concomitant with an increase of MD and a loss of FA in the cerebellum in MSA-C patients compared with MSA-P patients. This result is in agreement with previous MR results⁴² and the predominant clinical syndrome.

Limits

Longitudinal studies on large cohorts of patients with MSA and PD patients will be crucial to confirming our results and to accurately following brain modifications from Parkinson's disease progression. Although the sample size in the current study was within the accepted range for published studies (eg, reference 10), we acknowledge that results from a sample of this size must be taken with caution and may not generalize to the whole population studied. The sequences used in this mMRI study have been chosen to design a clinically practical method that can be implemented on whatever 3T MR scanners.

Conclusions

The main contribution of our multiparametric MRI approach was higher discrimination power between patients with disorders and HCs than in previous studies.^{8,9} Additional studies are needed to confirm that without the availability of any a priori information supplied by the operator, mMRI can improve the differential diagnosis between MSA and PD, also in the early stages, when the clinical diagnosis remains challenging. Future studies may include new MRI techniques that have been demonstrated to be sensitive to parkinsonian-related changes and to have intrinsically high discriminant power such as QSM²⁷ and free-water imaging.¹⁰ ■

Acknowledgments: We thank the Centre d'Investigation Clinique (CIC) for the global coordination of the clinical study and the Inserm/UPS UMR1214 Technical Platform for the MRI acquisitions.

References

- Halliday GM, Holton JL, Revesz T, et al. Neuropathology underlying clinical variability in patients with synucleinopathies. *Acta Neuropathol* 2011;122:187-204.
- Gilman S, Wenning GK, Low PA, et al. Second consensus statement on the diagnosis of multiple system atrophy. *Neurology* 2008;71:670-676.
- Berg D, Steinberger JD, Warren Olanow C, et al. Milestones in magnetic resonance imaging and transcranial sonography of movement disorders. *Mov Disord* 2011;26:979-992.
- Martin WRW, Wieler M, Gee M. Midbrain iron content in early Parkinson disease: A potential biomarker of disease status. *Neurology* 2008;70:1411-1417.
- Péran P, Cherubini A, Assogna F, et al. Magnetic resonance imaging markers of Parkinson's disease nigrostriatal signature. *Brain* 2010;133:3423-3433.
- Vaillancourt DE, Spraker MB, Prodoehl J, et al. High-resolution diffusion tensor imaging in the substantia nigra of de novo Parkinson disease. *Neurology* 2009;72:1378-1384.
- Meijer FJA, Aerts MB, Abdo WF, et al. Contribution of routine brain MRI to the differential diagnosis of parkinsonism: a 3-year prospective follow-up study. *J Neurol* 2012;259:929-935.
- Scherfler C, Göbel G, Müller C, et al. Diagnostic potential of automated subcortical volume segmentation in atypical parkinsonism. *Neurology* 2016;86:1242-1249.
- Huppertz H-J, Möller L, Südmeyer M, et al. Differentiation of neurodegenerative parkinsonian syndromes by volumetric magnetic resonance imaging analysis and support vector machine classification. *Mov Disord* 2016;0:1-12.
- Planetta PJ, Ofori E, Pasternak O, et al. Free-water imaging in Parkinson's disease and atypical parkinsonism. *Brain* 2016;139:495-508.
- Hughes AJ, Daniel SE, Kilford L, et al. Accuracy of clinical diagnosis of idiopathic Parkinson's disease: a clinico-pathological study of 100 cases. *J Neurol Neurosurg Psychiatry* 1992;55:181-184.
- Hoehn MM, Yahr MD. Parkinsonism: onset, progression, and mortality. 1967. *Neurology* 2001;57:S11-S26.
- Tomlinson CL, Stowe R, Patel S, et al. Systematic review of levodopa dose equivalency reporting in Parkinson's disease. *Mov Disord* 2010;25:2649-2653.
- Fahn S ERUDC. The Unified Parkinson's Disease Rating Scale; 1987.
- Péran P, Cherubini A, Luccichenti G, et al. Volume and iron content in basal ganglia and thalamus. *Hum Brain Mapp* 2009;30:2667-2675.
- Cherubini A, Péran P, Caltagirone C, et al. Aging of subcortical nuclei: microstructural, mineralization and atrophy modifications measured in vivo using MRI. *Neuroimage Published Online First*; 2009.
- Winkler AM, Ridgway GR, Webster MA, et al. Permutation inference for the general linear model. *Neuroimage* 2014;92:381-397.
- Smith SM, Nichols TE. Threshold-free cluster enhancement: Addressing problems of smoothing, threshold dependence and localisation in cluster inference. *Neuroimage* 2009;44:83-98.
- Litvan I, Bhatia KP, Burn DJ, et al. Movement Disorders Society Scientific Issues Committee report: SIC Task Force appraisal of clinical diagnostic criteria for parkinsonian disorders. *Mov Disord* 2003;18:467-486.
- Osaki Y, Ben-Shlomo Y, Lees AJ, et al. A validation exercise on the new consensus criteria for multiple system atrophy. *Mov Disord* 2009;24:2272-2276.
- Petrovic IN, Ling H, Asi Y, et al. Multiple system atrophy-parkinsonism with slow progression and prolonged survival: A diagnostic catch. *Mov Disord* 2012;27:1186-1190.
- Meissner WG, Laurencin C, Tranchant C, et al. Outcome of deep brain stimulation in slowly progressive multiple system atrophy: a clinico-pathological series and review of the literature. *Parkinsonism Relat Disord* 2016;24:69-75.
- Barbagallo G, Sierra-Peña M, Nemmi F, et al. Multimodal MRI assessment of nigro-striatal pathway in multiple system atrophy and Parkinson disease. *Mov Disord* 2016;31:325-334.

24. Dexter DT, Carayon A, Javoy-Agid F, et al. Alterations in the levels of iron, ferritin and other trace metals in Parkinson's disease and other neurodegenerative diseases affecting the basal ganglia. *Brain* 1991;114(Part 4):1953-1975.
25. Sofic E, Paulus W, Jellinger K, et al. Selective increase of iron in substantia nigra zona compacta of parkinsonian brains. *J Neurochem* 1991;56:978-982.
26. Baudrexel S, Nürnberger L, Rüb U, et al. Quantitative mapping of T1 and T2* discloses nigral and brainstem pathology in early Parkinson's disease. *Neuroimage* 2010;51:512-520.
27. Langkammer C, Pirpamer L, Seiler S, et al. Quantitative Susceptibility Mapping in Parkinson's Disease. *PLoS One* 2016;11:e0162460.
28. Reiter E, Mueller C, Pinter B, et al. Dorsolateral nigral hyperintensity on 3.0T susceptibility-weighted imaging in neurodegenerative Parkinsonism. *Mov Disord* 2015;30:1068-1076.
29. Langley J, Huddleston DE, Merritt M, et al. Diffusion tensor imaging of the substantia nigra in Parkinson's disease revisited. *Hum Brain Mapp* 2016;37:2547-2556.
30. Schwarz ST, Abaei M, Gontu V, et al. Diffusion tensor imaging of nigral degeneration in Parkinson's disease: A region-of-interest and voxel-based study at 3 T and systematic review with meta-analysis. *Neuroimage Clin* 2013;3:481-488.
31. Brenneis C, Seppi K, Schocke MF, et al. Voxel-based morphometry detects cortical atrophy in the Parkinson variant of multiple system atrophy. *Mov Disord* 2003;18:1132-1138.
32. Tir M, Delmaire C, le Thuc V, et al. Motor-related circuit dysfunction in MSA-P: usefulness of combined whole-brain imaging analysis. *Mov Disord* 2009;24:863-870.
33. Focke NK, Helms G, Pantel PM, et al. Differentiation of typical and atypical Parkinson syndromes by quantitative MR imaging. *AJNR Am J Neuroradiol* 2011;32:2087-2092.
34. Lee J-H, Baek S-Y, Song Y, et al. The neuromelanin-related T2* contrast in postmortem human substantia nigra with 7T MRI. *Sci Rep* 2016;6:32647.
35. Nicoletti G, Rizzo G, Barbagallo G, et al. Diffusivity of cerebellar hemispheres enables discrimination of cerebellar or parkinsonian multiple system atrophy from progressive supranuclear palsy-Richardson syndrome and Parkinson disease. *Radiology* 2013;267:843-850.
36. Worker A, Blain C, Jarosz J, et al. Diffusion tensor imaging of Parkinson's disease, multiple system atrophy and progressive supranuclear palsy: a tract-based spatial statistics study. *PLoS One* 2014;9:e112638.
37. Pellecchia MT, Barone P, Mollica C, et al. Diffusion-weighted imaging in multiple system atrophy: A comparison between clinical subtypes. *Mov Disord* 2009;24:689-696.
38. Nicoletti G, Fera F, Condino F, et al. MR Imaging of middle cerebellar peduncle width: differentiation of multiple system atrophy from Parkinson disease. *Radiology* 2006;239:825-830.
39. Paviour DC, Thornton JS, Lees AJ, et al. Diffusion-weighted magnetic resonance imaging differentiates Parkinsonian variant of multiple-system atrophy from progressive supranuclear palsy. *Mov Disord* 2007;22:68-74.
40. Wu Y-T, Shyu K-K, Jao C-W, et al. Quantifying cerebellar atrophy in multiple system atrophy of the cerebellar type (MSA-C) using three-dimensional gyrification index analysis. *Neuroimage* 2012;61:1-9.
41. Lee J-H, Han Y-H, Kang B-M, et al. Quantitative assessment of subcortical atrophy and iron content in progressive supranuclear palsy and parkinsonian variant of multiple system atrophy. *J Neurol* 2013;260:2094-2101.
42. Lee EA, Cho HI, Kim SS, et al. Comparison of magnetic resonance imaging in subtypes of multiple system atrophy. *Parkinsonism Relat Disord* 2004;10:363-368.

Supporting Data

Additional Supporting Information may be found in the online version of this article at the publisher's website.